

Enhanced water oxidation reaction kinetics on BiVO₄ photoanode by the surface modification with Ni₄O₄ cubane

Bin Gao^a, Tao Wang^{a,*}, Xiaoli Fan^a, Hao Gong^a, Peng Li^a, Yaya Feng^a,
Xianli Huang^a, Jianping He,^{a,*} Jinhua Ye^{b,*}

^a College of Materials Science and Technology, Jiangsu Key Laboratory of Electrochemical Energy Storage Technologies, Nanjing University of Aeronautics and Astronautics, Nanjing 210016, PR China.

^b International Center for Materials Nanoarchitectonics (WPI-MANA), National Institute for Materials Science (NIMS), 1-1 Namiki, Tsukuba, Ibaraki 305-0044 (Japan)

*Corresponding authors:

Prof. Tao Wang, Tel: +86 25 52112900; Fax: +86 25 52112626, E-mail:
wangtao0729@nuaa.edu.cn;

Prof. Jianping He, Tel: +86 25 52112900; Fax: +86 25 52112626, E-mail:
jianph@nuaa.edu.cn;

Prof. Jinhua Ye, Tel: +81 29 8592646; Fax: +81 29 8604958, E-mail:
Jinhua.YE@nims.go.jp.

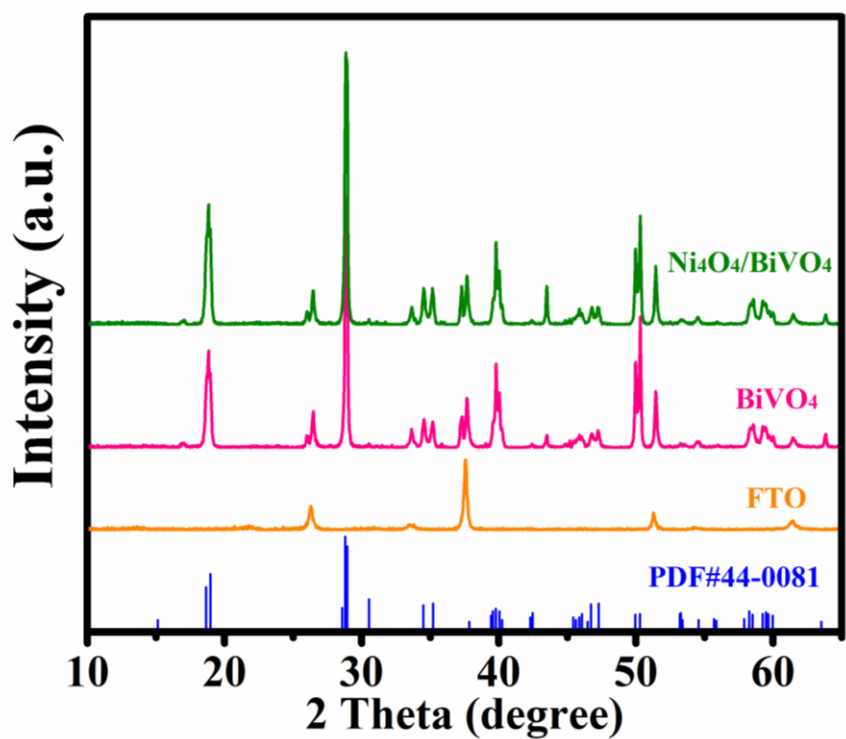


Fig. S1. XRD of Ni₄O₄/BiVO₄ and BiVO₄ photoanodes.

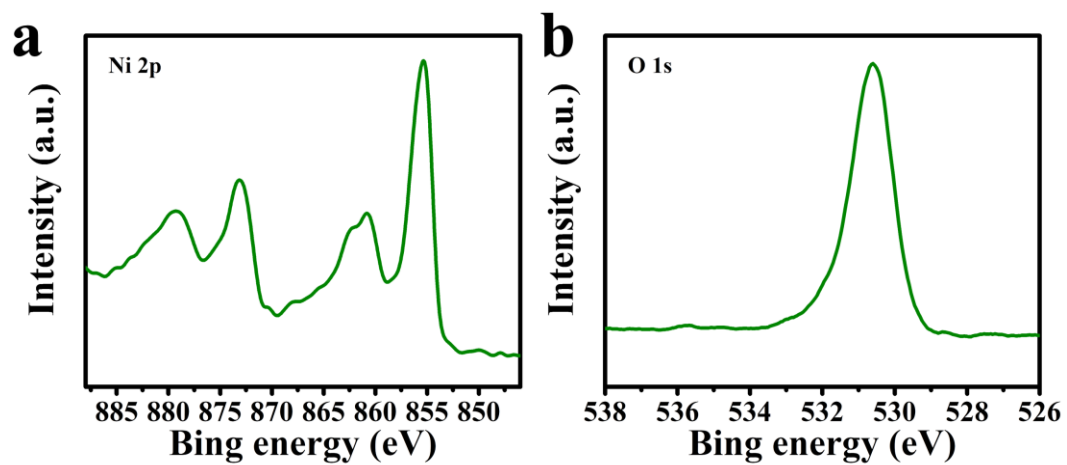


Fig. S2. High-resolution spectrum of Ni 2p (a) and O 1s (b) of $\text{Ni}(\text{OH})_2$.

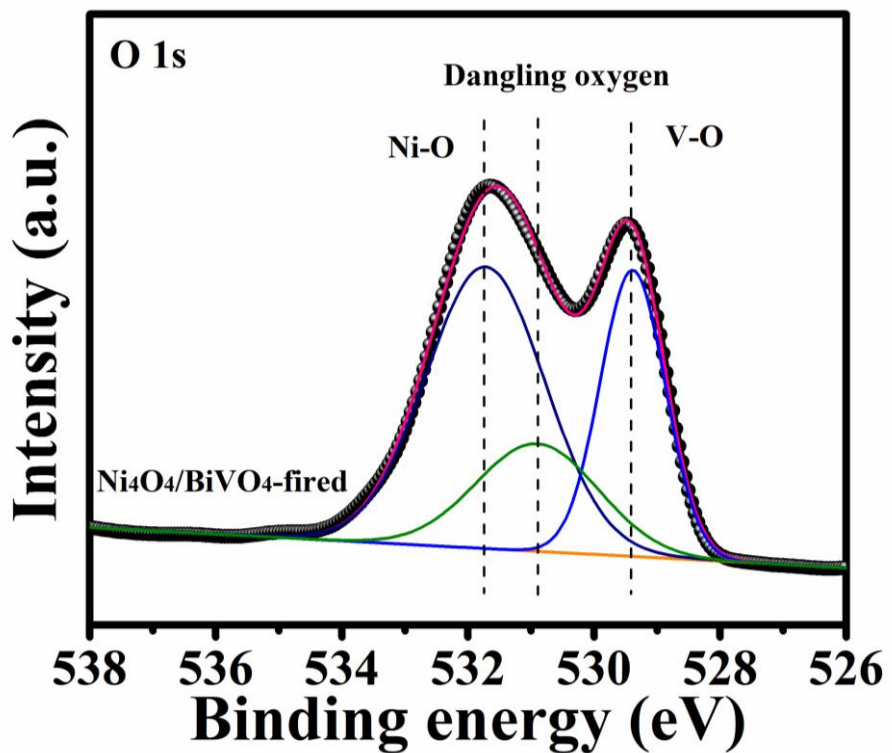


Fig. S3. High-resolution spectrum of O 1s of Ni₄O₄/BiVO₄ photoanode after fired.

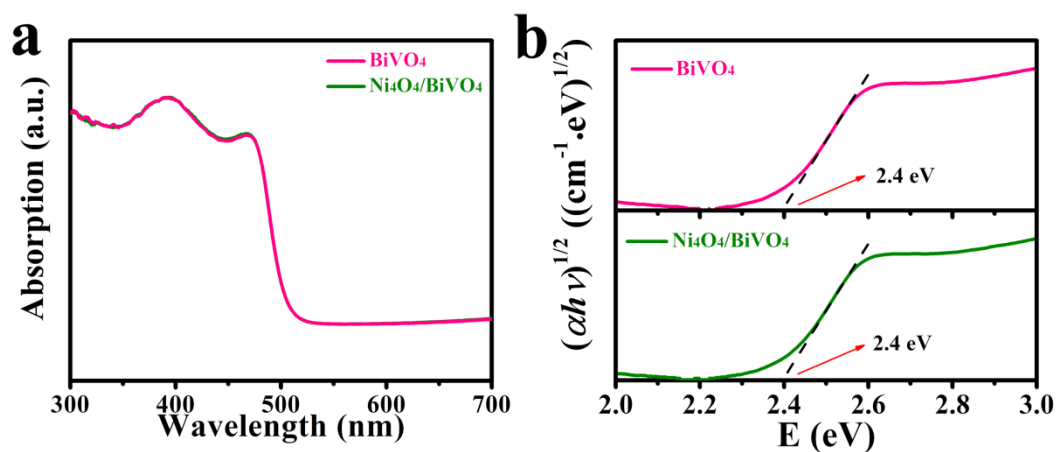


Fig. S4. UV-vis spectra (a) and tauc plots (b) of BiVO₄ and Ni₄O₄/BiVO₄.

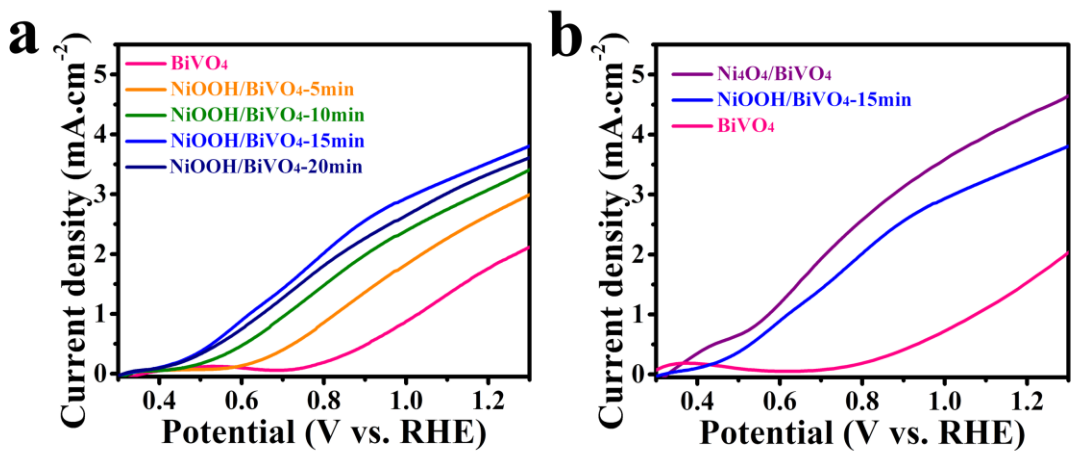


Fig. S5. (a) LSV of NiOOH modified BiVO_4 photoanodes with different deposition time; (b) LSV of $\text{Ni}_4\text{O}_4/\text{BiVO}_4$ and $\text{NiOOH}/\text{BiVO}_4$. Depositional condition: three-electrode system, 0.1 M NiSO_4 solution with pH adjusted to 7 by NaOH and a bias voltage of 1 V (vs. SCE)

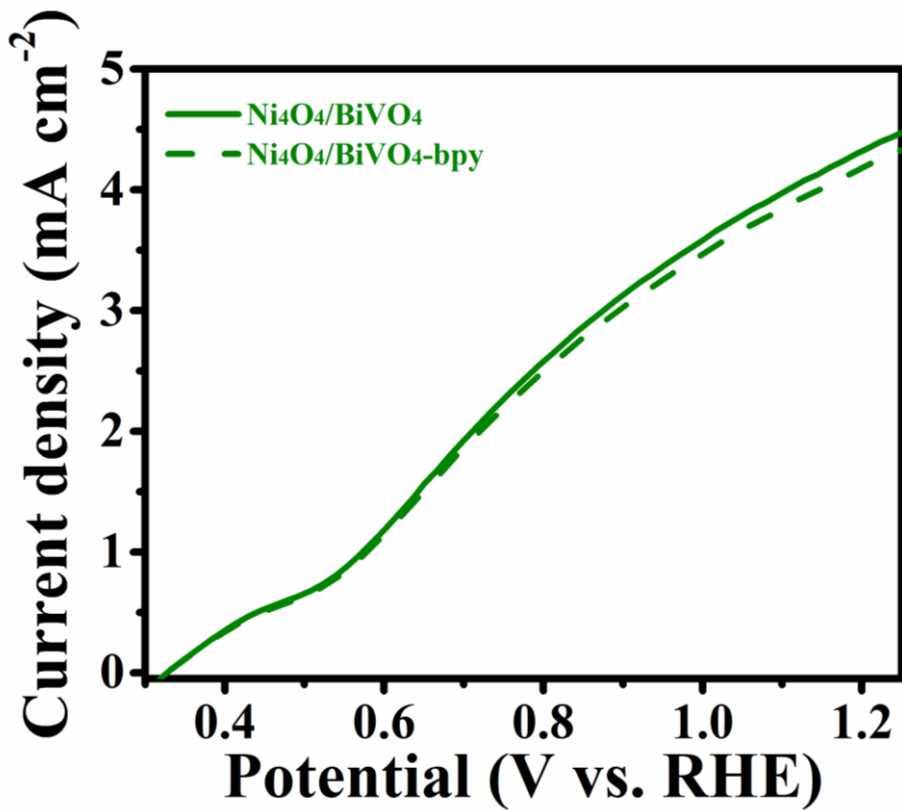


Fig. S6. LSV curves of $\text{Ni}_4\text{O}_4/\text{BiVO}_4$ in phosphate buffer electrolyte (pH=7) with 80 μM bpy and without bpy.

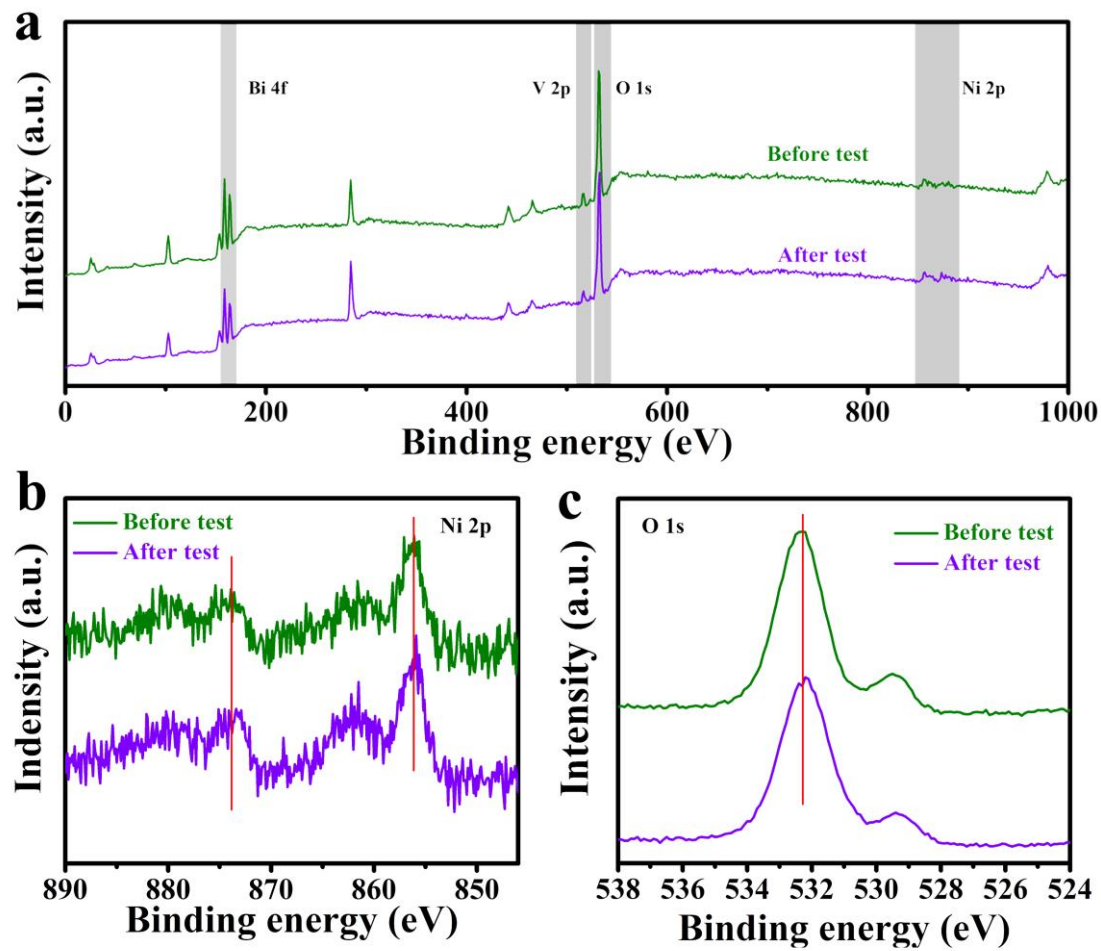


Fig. S7. XPS survey spectrum (a) and high- resolution spectra of Ni 2p (b), O 1s (c) of $\text{Ni}_4\text{O}_4/\text{BiVO}_4$ before and after testing.

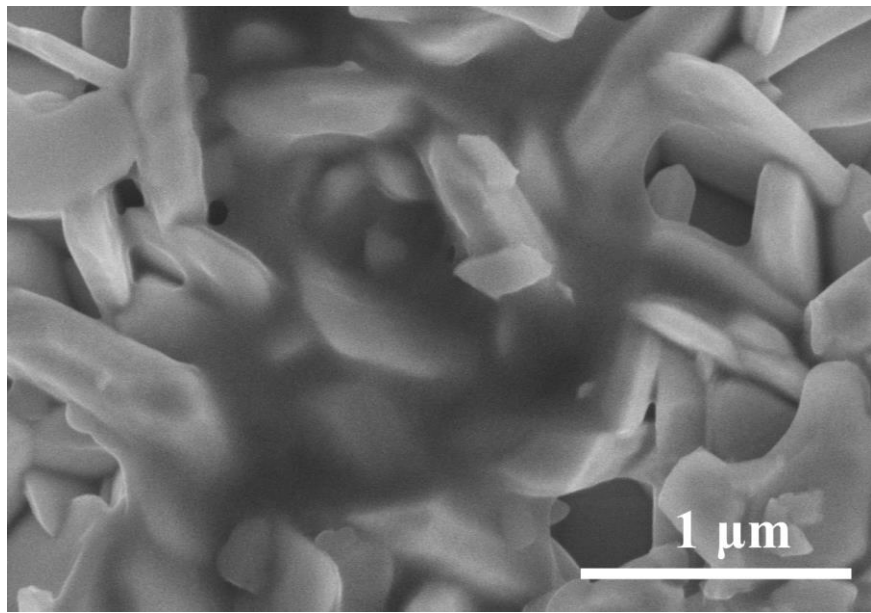


Fig. S8. The SEM image of $\text{Ni}_4\text{O}_4/\text{BiVO}_4$ photoanode after tested.

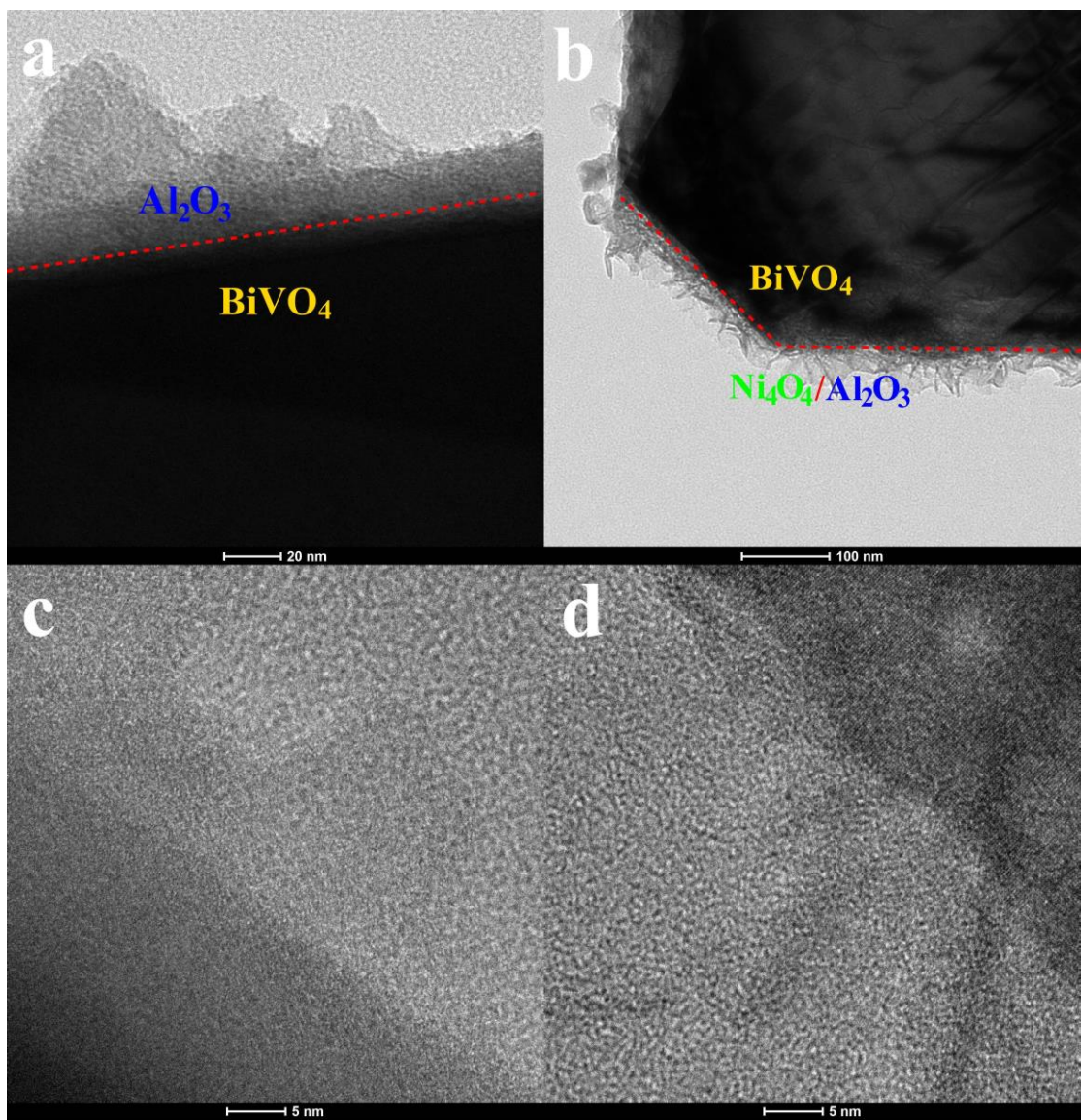


Fig. S9. The TEM and HRTEM images of $\text{Al}_2\text{O}_3/\text{BiVO}_4$ (a, c) and $\text{Ni}_4\text{O}_4/\text{Al}_2\text{O}_3/\text{BiVO}_4$ (b, d) nanoplate.

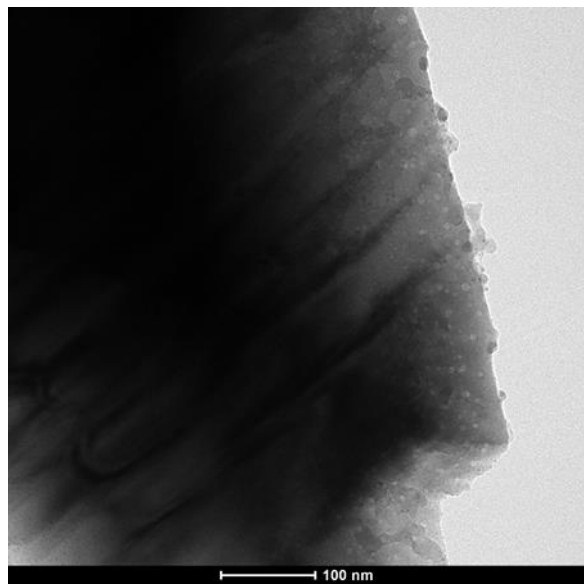


Fig. S10. The TEM image of BiVO_4 crystal.

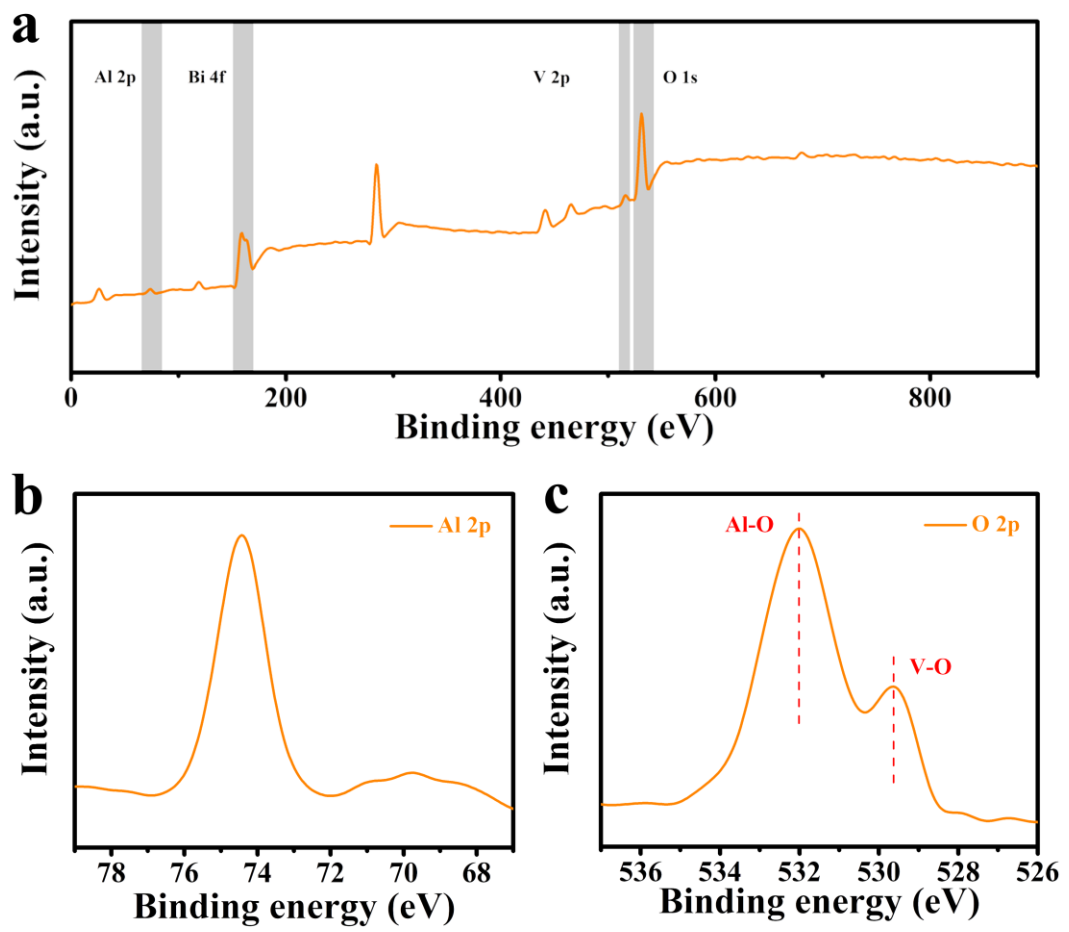


Fig. S11. XPS survey spectrum (a) and high resolution Al 2p (b) and O 2p (c) XPS spectra of $\text{Al}_2\text{O}_3/\text{BiVO}_4$ photoanode.

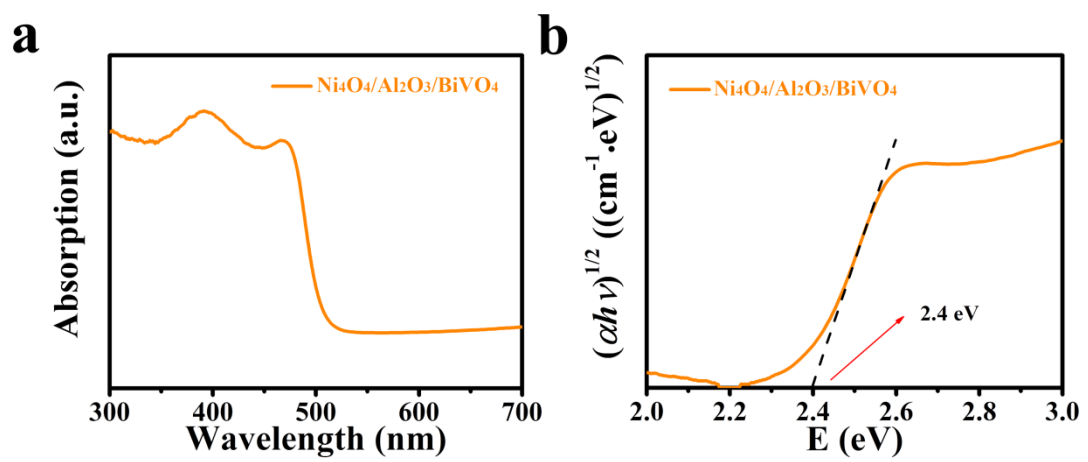


Fig. S12. UV-vis spectra (a) and tauc plots (b) of Al₂O₃/BiVO₄.

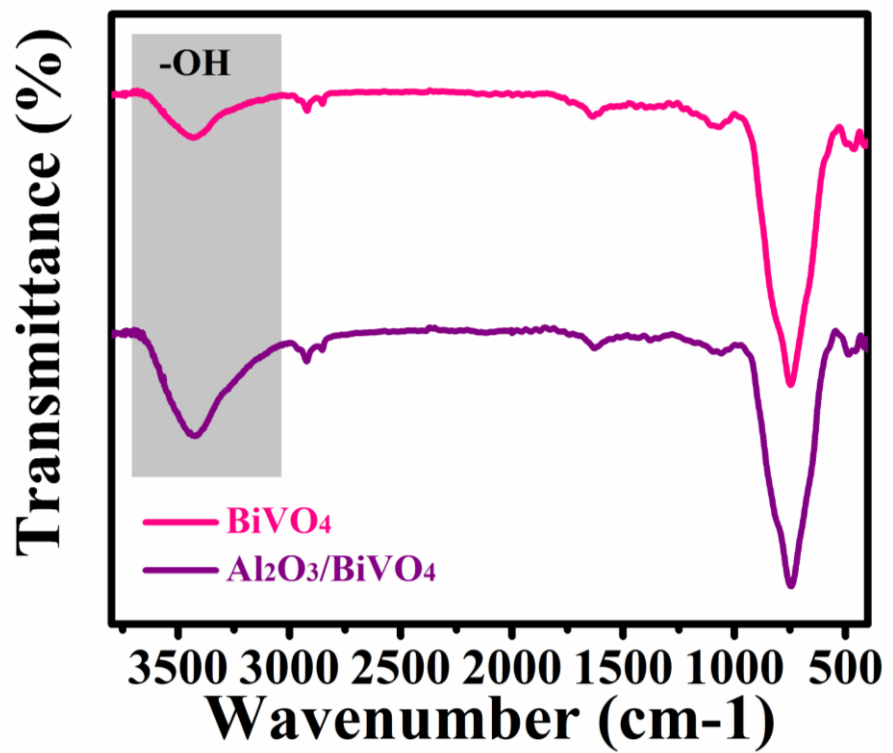


Fig. S13. FTIR of BiVO₄ and Al₂O₃/BiVO₄.

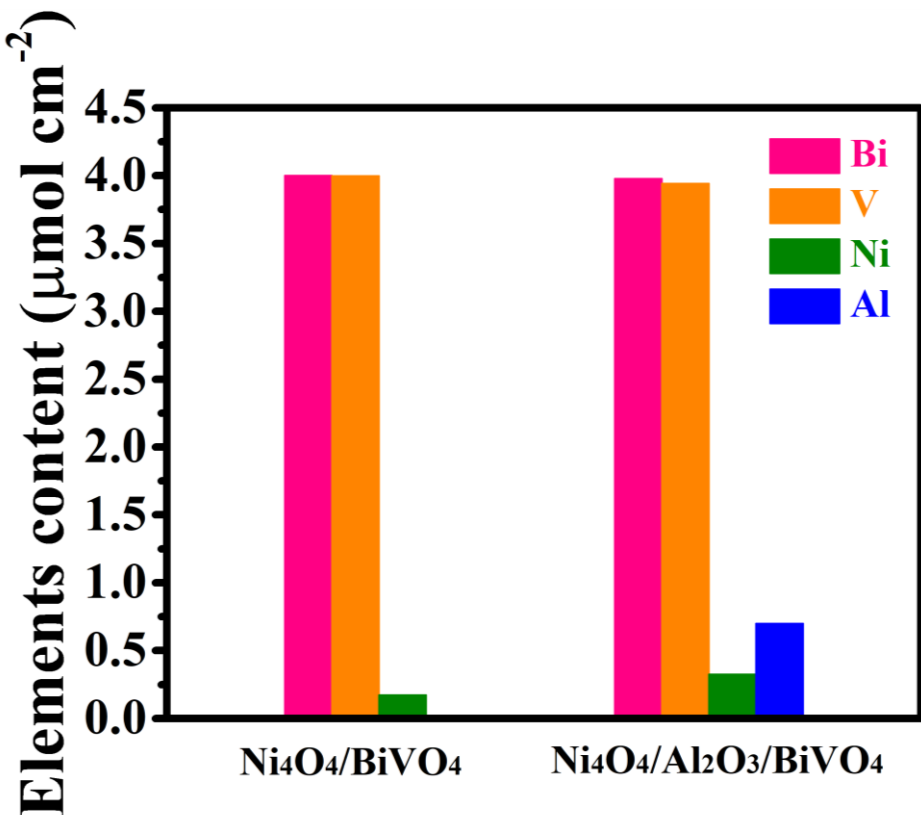


Fig. S14. ICP of $\text{Ni}_4\text{O}_4/\text{BiVO}_4$ and $\text{Ni}_4\text{O}_4/\text{Al}_2\text{O}_3/\text{BiVO}_4$.

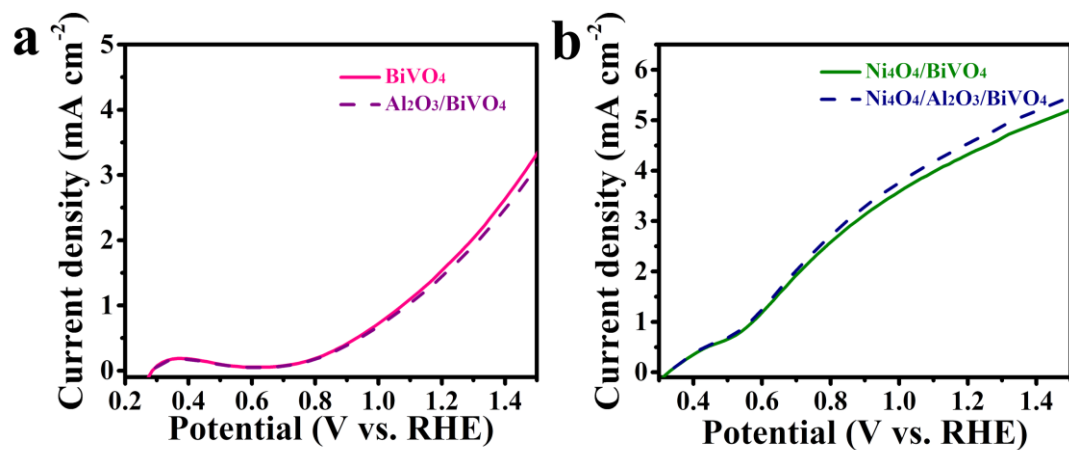


Fig. S15. The LSV curves of BiVO_4 and $\text{Al}_2\text{O}_3/\text{BiVO}_4$ (a) and $\text{Ni}_4\text{O}_4/\text{BiVO}_4$ and $\text{Ni}_4\text{O}_4/\text{Al}_2\text{O}_3/\text{BiVO}_4$ (b).

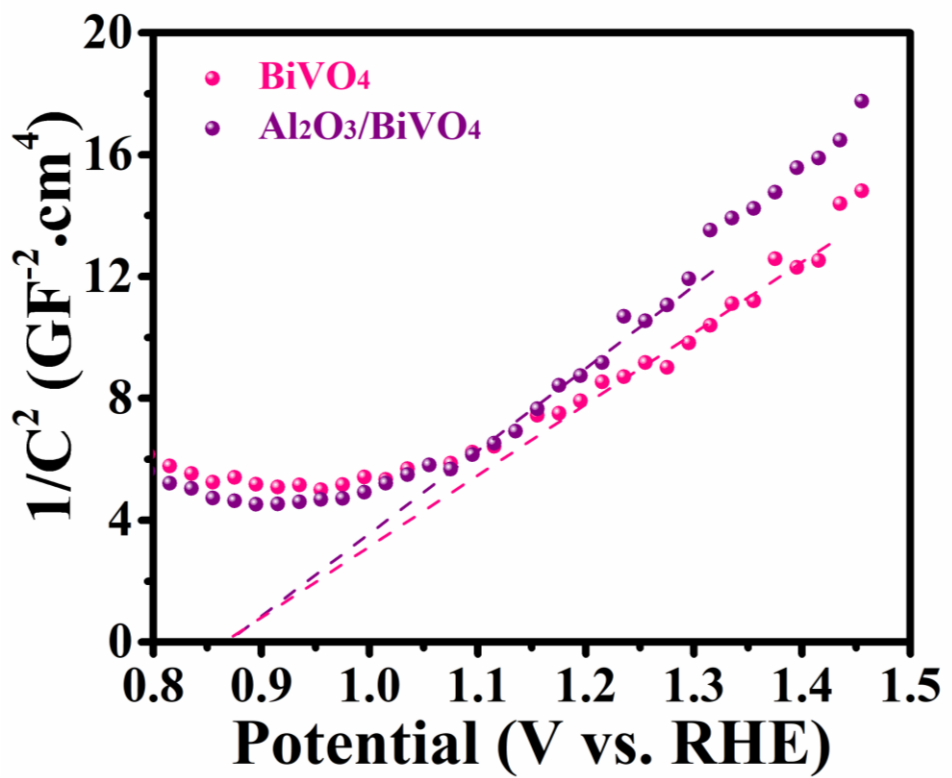


Fig. S16. Mott-schottky plots of BiVO₄ and Al₂O₃/BiVO₄ photoanode.

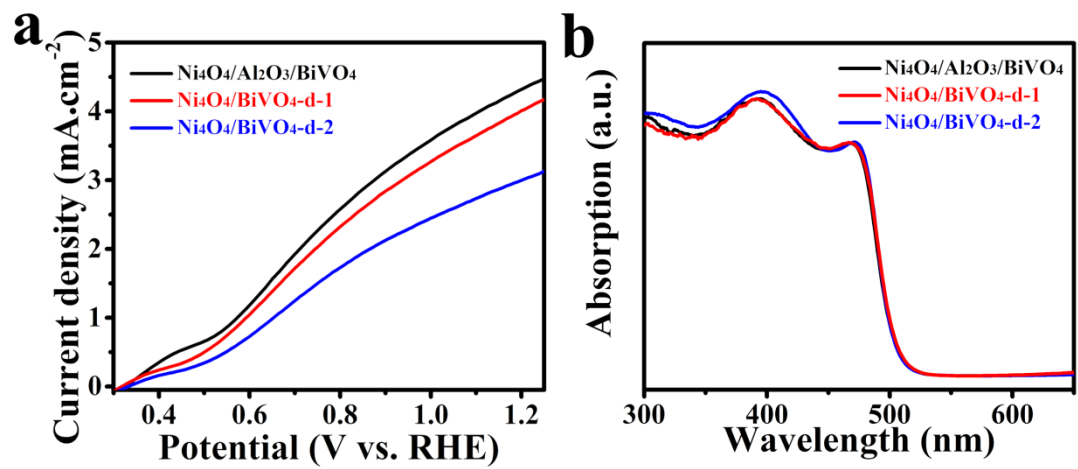


Fig. S17. (a) LSV and (b) UV-vis spectra of Ni₄O₄/Al₂O₃/BiVO₄, Ni₄O₄/BiVO₄-d-1 and Ni₄O₄/BiVO₄-d-2.

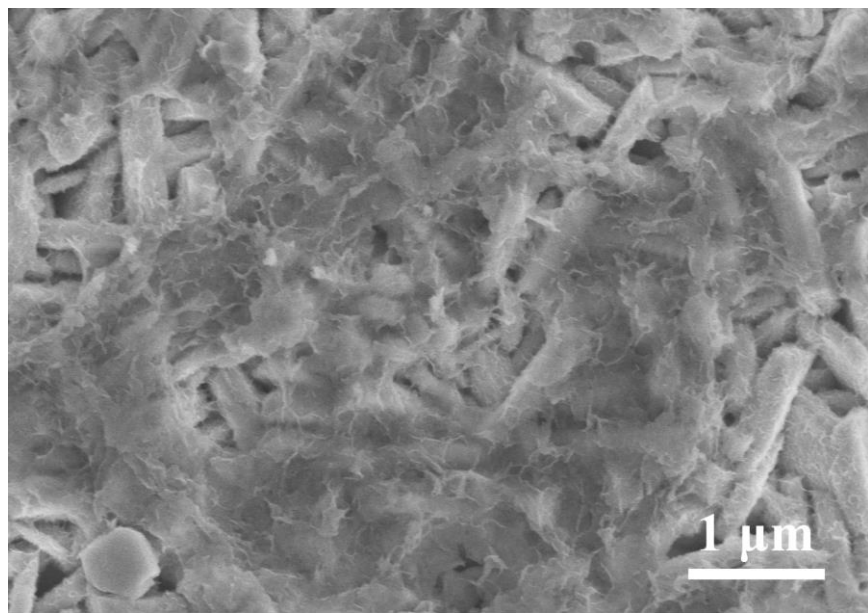


Fig. S18. The SEM image of $\text{Ni}_4\text{O}_4/\text{Al}_2\text{O}_3/\text{BiVO}_4$ photoanode after tested.

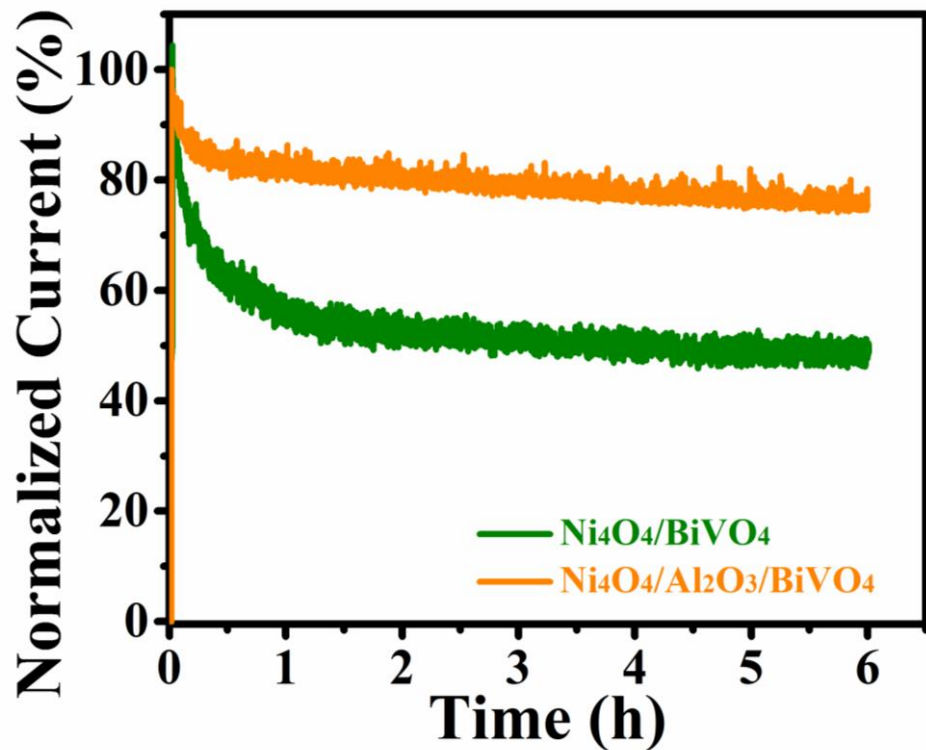


Fig. S19. I-t curve of $\text{Ni}_4\text{O}_4/\text{BiVO}_4$ and $\text{Ni}_4\text{O}_4/\text{Al}_2\text{O}_3/\text{BiVO}_4$ photoanodes for 6 h.

Table S1. Summary of the water oxidation properties of high performing OER catalysts for BiVO₄ based photoanodes.

Photoanode	Light source	Electrolyte	Onset potential with cocatalyst (V)	Onset potential without cocatalyst (V)	Photocurrent density with cocatalyst (mA/cm ⁻² , 1.23 VRHE)	Photocurrent density without cocatalyst (mA/cm ⁻² , 1.23 VRHE)	Ref.
Ni ₄ O ₄ /BiVO ₄	AM	0.5 M KPi*					This work
	1.5G	(pH=7)	0.35	0.7	3.9	1.5	
FeOOH/NiOOH /BiVO ₄	AM	0.5 M KPi					1
	1.5G	(pH=7)	0.23	0.43	4.2	1.8	
NiO/CoO _x /BiV _{O₄}	AM	0.1 M KPi					2
	1.5G	(pH=7)	0.35	0.55†	3.5	1.05†	
CoFe-H/BiVO ₄	AM	0.5 M KPi					3
	1.5G	(pH=7)	0.23	0.68	2.48	0.78	
β-FeOOH/BiVO ₄	AM	0.2 M Na ₂ SO ₄					4
	1.5G		0.45†	0.65†	4.3	1.45†	
NiB/BiVO ₄	AM	0.5 M KB**					5
	1.5G	(pH=9.2)	0.25	0.35	3.47	1.56	
Co ₃ O ₄ /BiVO ₄	AM	1 M KB					6
	1.5G	(pH=9.5)	0..55	Unconspicuous	2.71	0.71	
CoPi/BiVO ₄	365 nm						7
	LEDs	0.1 M KPi					
	(AM	(pH=6.7)	0.5	0.9	2	0.9	
	1.5G)						

* KPi: Potassium phosphate buffer

** KB: Potassium borate buffer

† Estimated from figures in reference, unless denoted otherwise

Tab. S2. Calculated and measured gas evolution rates obtained from Fig. 8 (data during the first hour).

	O ₂ evolution rate ($\mu\text{mol h}^{-1}$)	Photocurrent density (mA cm^{-2})	Faradaic efficiency (%)
Actual	31.2	3.34	96.3
Theoretical	32.4	3.47	100

References

- [1] T. W. Kim, K. S. Choi, *Science*, 2014, **45**, 990-994.
- [2] M. Zhong, T. Hisatomi, Y. Kuang, J. Zhao, M. Liu, A. Lwase, Q. Jia, H. Nishiyama, T. Minegishi, M. Nakabayashi, N. Shibata, R. Nishiro, C. Katayama, H. Shibano, M. Katayama, A. Kudo, T. Yamada, K. Domen, *J. Am. Chem. Soc.*, 2015, **137**, 5053-5060.
- [3] W. Liu, H. Liu, L. Dang, H. Zhang, X. Wu, B. Yang, Z. Li, X. Zhang, L. Lei, S. Jin, *Adv. Funct. Mater.*, 2017, **27**, 1603904.
- [4] B. Zhang, L. Wang, Y. Zhang, Y. Ding, Y. Bi, *Angew. Chem. Int. Edit.*, 2018, **57**, 2248-2252.
- [5] K. Dang, X. Chang, T. Wang, J. Gong, *Nanoscale*, 2017, **9**, 16133-16137.
- [6] X. Chang, T. Wang, P. Zhang, J. Zhang, A. Li, J. Gong, *J. Am. Chem. Soc.*, 2015, **137**, 8356-8359.
- [7] Y. Ma, A. Kafizas, S. R. Pendlebury, F. L. Formal, J. R. Durrant, *Adv. Funct. Mater.*, 2016, **26**, 4951-4960.